



Applying a network of high frequency ultrasonic transducers for removal of Reactive Red 120 dye from aqueous solution: experimental design and statistical analysis

Sajad Khorshidi, Akbar Mohammadidoust*

Department of Chemical Engineering, Kermanshah Branch, Islamic Azad University, Kermanshah, Iran

ARTICLE INFO

Article history:

Received 5 October 2020

Received in revised form

26 February 2021

Accepted 8 March 2021

Keywords:

Reactive Red 120

Ultrasonic transducer's network

Optimization

Response surface methodology

Artificial neural network

ABSTRACT

In this study a network of high frequency ultrasonic's transducers without additives was introduced for removing the Reactive Red 120 dye from aqueous solution. pH, irradiation time, initial concentration and number of piezoelectric were input variables at constant temperature of 25 °C. The results revealed that the ultrasonic waves played an important role in cracking the hydrocarbon bonds due to the cavitation phenomenon and OH[•] attacks. The effects of the variables and their interactions were investigated by the central composite design (CCD) method as one of the response surface methodologies (RSM). Maximum dye removal's efficiency (76.05%) was attained at initial concentration of 5 mg/l, irradiation time of 50 min; pH 10 and 5 ultrasonic's transducers. It was in a good agreement with the experimental, 78%. Finally, to more evaluates, the RSM model was compared to the artificial neural network (ANN) model. Performance's functions reported that the RSM was better than the ANN in predicting the dye removal's efficiency (R%).

1. Introduction

Water is one of the most essential elements of life on earth. Clean and safe water is considered as a major issue facing mankind. Nowadays water consumption is gradually increasing and different pollutants diffuse into water sources through various ways. They will make a critical condition in the future [1]. Some wastewaters contain dangerous substances that are chemically and biologically stable [1]. In recent decades, due to the ever expanding industries, produced wastewater has significantly grown. The release of toxic and harmful contaminants including dyes and phenolic compounds into the environment has made an undesirable change in the ecosystem. The dyes of the textile wastewater and related industries are one of the large groups of polluting organic compounds [1,2]. Therefore, decolorization's processes have attracted the attention of researchers in order to reach an optimum response [2-7]. Removal of dyes and pigments can be to some extent useful through the conventional processes such as the adsorption, filtration, reverse osmosis,

coagulation, deposition and etc. [8-11]. These methods only transfer organic compounds from the effluent to other phase, resulting in secondary pollution and high cost. In addition, because of the large size of the aromatics in the dye's molecules and stability of the new dyes, the conventional biological methods have no significant effect [12-15]. When the azo dyes make the bio-resistant toxic aromatics, applying the advanced oxidation processes (AOPs) can be effective in cracking dyes' molecules as efficient novel approaches. In general, AOPs degrade the organic pollutants by using very active species, e.g. hydroxyl radicals [16-19]. For instance, Fenton and electro-Fenton processes have been employed by many researchers [20-25]. In 2009, removal of green B dye was carried out through the electro-Fenton process in a bubble reactor. Removal's efficiency of 80% occurred at optimum conditions within 21 h [26]. Moreover, in 2011, a fluidized bed reactor was used to eliminate of dye from the textile wastewater. In an acidic solution, 92% of dye's removal was attained after 2 min [27]. Photo-oxidation processes are

*Corresponding author. Tel: +98-918913707

Email address: mohammadidoust@gmail.com

DOI: 10.22104/AET.2021.4443.1241

other AOPs which are well effective in cracking of hydrocarbon bonds [28-33]. In 2009, combining UV/SO was implemented for removing the dye with a high efficiency. Maximum dye's removal was found by 84% at optimum parameters. The results showed that combining UV/SO was better than UV and SO, alone, in decreasing the dye's concentration [34]. In another work, the biological method was employed for removing the cango red dye. The enzyme of *oudemansiella canarii* could remove the dye by 80% at 50 mg/l of cango red within 24 h at 30 °C and pH 5.5 [35]. Also, Carmoisine as an azo dye was removed by *saccharomyces cerevisiae* ATCC 9763. 50 mg/l of carmoisine was eliminated after 7 h of incubation at optimum conditions [36]. As mentioned above, there are several methods for eliminating the azo dyes. The AOPs and the biological methods can be applicable in the industries. Recently ultrasonic waves' irradiation as one of the AOPs is capable to crack of the hydrocarbon bonds with a high quality and low cost. Mohammadidoust *et al.* used the ultrasonic waves in decreasing the kinematic viscosity of residue fuel oil. The results of that work revealed that the ultrasonic waves had a powerful effect in cracking the hydrocarbon's linkages [37]. In 2018, a heterogeneous sono-Fenton like was investigated on removal of azo dye RO 107. Complete elimination of the azo dye was attained at 0.8 g/l of nanoparticles, pH = 5, 10 mM of H₂O₂, 300 w/l of ultrasonic power and 25 min of reaction time [38]. In 2020, Shojaei *et*

al. [39] applied nanozeolite-X for removing three dyes. They could attain up to 93% of the dye mixture removal at optimum conditions in presence of ultrasonic irradiation. In addition, Shaikh *et al.* in 2021 [40] used biochar-based silver nanocomposite (Ag-nBC) for removing toxic dyes. The results of that work showed that synthesized adsorbent had a high potential in removing the dyes up to 90% at optimum conditions. Moreover, the acid orange 7 dye was removed due to packed-bed bioreactor by Swain *et al.* [41]. They proved that polyurethane foam (PUF) carriers played an important role in the dye removal. In that study, the maximum dye's removal of 87.31% and the chemical oxygen demand (COD) removal of 73.6% were attained at optimum conditions. Therefore, applying high frequency ultrasonic's waves to remove the azo dyes has rarely been studied in literature. Decolorization's process without additives can be cost-effective in many industries. In this work, different powers of ultrasonic waves at 1.7 MHz were employed for removal of the Reactive Red 120 (RR 120) in a network. The main aim of this study is to use the ultrasonic waves as a safe, low cost and fast approach to decrease the azo dye's concentration without additives. In addition, modeling, statistical analysis and optimization of the parameters are also the other purposes of the work. Finally, the optimized ramps of this work due to response surface methodology (RSM) are according to Figure 1.

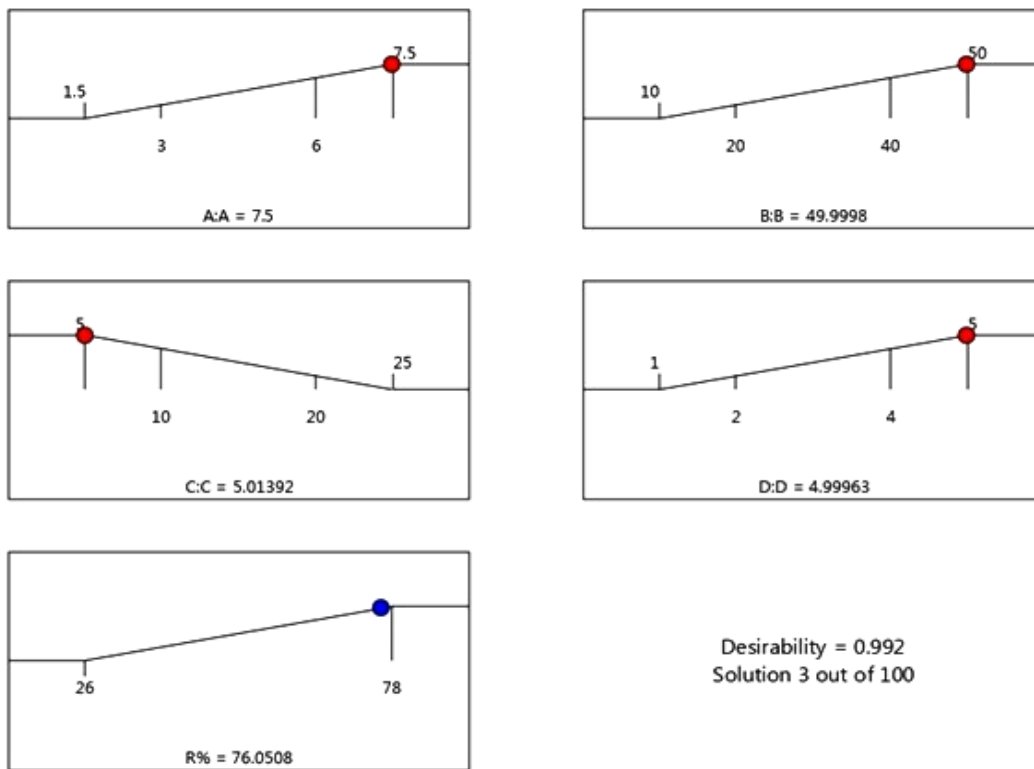


Fig. 1. Optimized ramps based on the RSM.

2. Materials and methods

2.1. Set up

The schematic view of the experimental set up is illustrated in Figure 2. Amount of 1 l of the Reactive Red 120 (RR120) dye with different concentrations was prepared and transferred into a cylindrical beaker with a volume of 3 l. Five piezoelectrics, cylindrical shape, were mounted in the container. The transducers (CTO11545, US) with a constant frequency of 1.7 MHz and maximum power of 10 W were employed. According to the laboratory results and optimization, a power of 10 W and configuration of two piezoelectrics on the bottom and three other on the

internal surface of the container were selected. The top of the container was closed and setting temperature was carried out by a cold bath at 15 ± 1 °C.

2.2. Materials

The RR120 diazo dye ($C_{44}H_{24}Cl_2N_{14}Na_6O_{20}S_6$, Mw = 1469.98 g/mol) was supplied from Sigma Co. The chemical structure is shown in Figure 3. The stock solutions were obtained by measuring specified mass of the dye into deionized water. In addition, pH adjustment of the solution was done through sulfuric acid and sodium hydroxide (Merck Inc.). All of materials in this work were of AR grade.

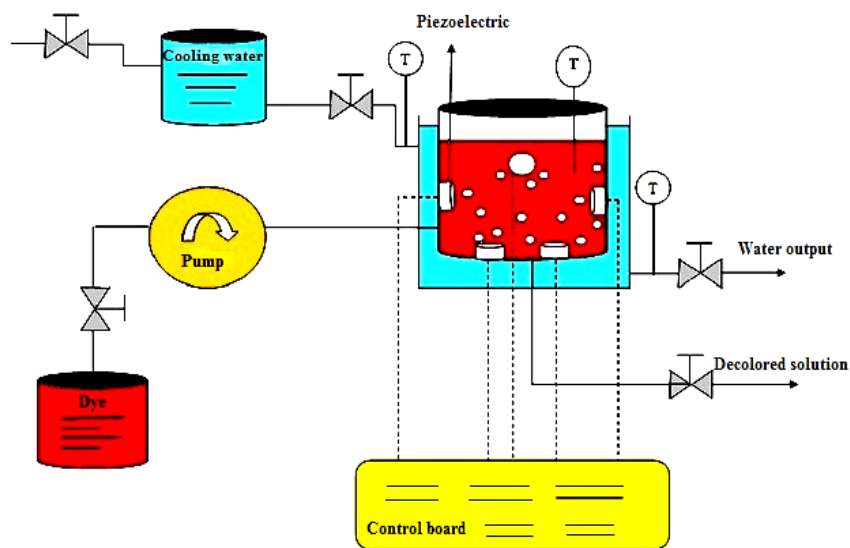


Fig. 2. Schematic view of experimental rig.

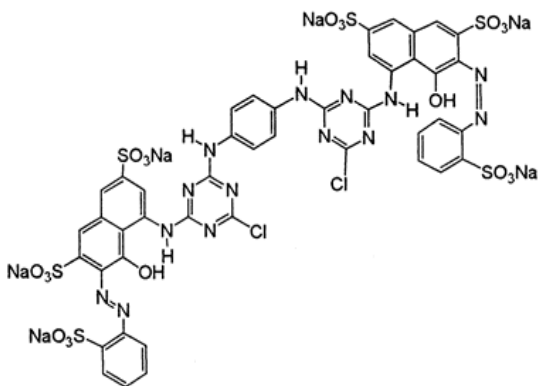


Fig. 3. Molecular structure of RR120 dye.

2.3. Procedure and analysis

The experiments of the process were conducted by a network of ultrasonic waves in a 3 l of container with specified architecture which was explained earlier. A volume of 1 l of the RR120 dye with different concentrations of 5-25 mg/l with step 5 was prepared from the stock solution. The solutions were injected to the beaker under known pH (1.5-7.5, step 1.5) that were measured by a pH

meter (Metrohm 827, Swiss) through 0.1 M H_2SO_4 or 0.1 M NaOH. The RR120 dye's solution was ultrasonically irradiated for different time intervals (10- 50 min, step 10). First the process of the dye's removal was implemented by one transducer (10 W) then the number of transducers was increased up to 5 based on the configuration in Figure 2. As mentioned about the range of the variables, design of experiments determined 30 experiments based on the central composite design (CCD). They have been reported according to Table 1. After each experiment due to its variables' level, the concentrations of the azo dye's samples were measured at 25 °C by a spectrophotometer (UV 2100, China). In UV apparatus, first blank and examined sample were placed in the specified cells and subsequently in their places. Then the wavelength was adjusted at λ_{max} of 508 nm due to the experimental results. After scanning and creating the related peak, the final concentration was determined based on the calibration curve and its absorption percent. This curve was drawn in terms of specified concentrations, previously. All of the experiments were analyzed in duplicate to obtain an exact value (average of the values).

The efficiency of the dye's removal (R) as the response of the statistical analysis was calculated as follows:

$$R\% = \left(\frac{C_0 - C}{C_0} \right) 100 \quad (1)$$

Where, C_0 and C are the initial and final concentrations of the dye in the solution (mg/l) respectively. The experimental data were analyzed by response surface methodology. In addition, analysis of variance (ANOVA) and a quadratic model were studied, completely. Finally, the RSM and ANN models were compared and validated.

3. Data analyses

3.1. Response surface methodology (RSM)

Response surface methodology plays a significant role in designing experiments and statistical analysis of data. The RSM evaluates many complex processes which have not been introduced through clear relationships among parameters. It assesses the effects of the linear, second order and interaction between parameters with a high accuracy. The ARM including two main approaches; Box-Behnken design (BBD) and Central composite design (CCD) [42]. Forecasting the optimum conditions due to the experimental data is very prominent in obtaining maximum or minimum responses in the processes. In the past, using univariate method was neither precise nor general. Therefore applying the statistical methods can be effective in analyzing interactions and non-linear effects of variables. The RSM has a crucial effect in complete study of the process by combining the mathematical and statistical methods [42,43]. In brief, the RSM consists of three steps; design of experiment, modeling and optimization which investigate variables in three main levels (low (-1), medium (0), high (+1)) [43]. Decreasing cost, time and number of experiments are the advantages of this method. In addition, determining the significance degree of the variables in processes, alone and interaction, and introducing a quadratic model (Appendix A) are other preferences. In this work, Design Expert software ver.12 was employed.

3.2. Artificial neural network (ANN)

To evaluate, compare and validate the RSM results, the powerful tool of the artificial intelligence was used. Artificial neural network as one of the subsets of the artificial intelligence is capable in developing complex processes with different independent variables. The MATLAB software (R2014a) used to model the efficiency of the dye's removal versus the independent variables. In summary, the ANN model's architecture includes input, hidden and output layers which have some neurons. The neurons of each layer are linked by the known layers and a continuous group was produced by the weights and biases. Then, a logical pattern between inputs and outputs was made. The ANN considers the number of inputs and outputs

as neurons of the input and output layers, respectively, while number of neurons in the hidden layer is estimated by trial-and-error method [44]. The ANN consists of several network types as Feed-forward back propagation, Elman back propagation, Cascade-forward back propagation, Competitive and so on. In this work, the feed-forward back propagation was employed with a high precision compared to the other network types. This network's type has several algorithms including trainlm (Levenberg-Marquardt), trainbr (Bayesian Regulation), traincgb (Conjugate Gradient with Beale-Powell Restarts), trainrp (Random Propagation), trainscg (Scaled Conjugate Gradient), etc [44]. The ANN makes the suitable weights and biases and utilizes in an equation due to number of neurons and transfer functions of the hidden and output layers (Appendix A). The "tansig" and "purelin" were considered as the conventional transfer functions in the layers.

4. Results and discussion

4.1. Design of experiments (DOE)

4.1.1. Response surface methodology (RSM)

In this work, the CCD as a subset of the RSM was employed to clarify the effects of the variables in the decolorization of the RR120 dye. The CCD had a higher accuracy than the BBD in the statistical analyses of the experimental data. The pH, initial concentration of the dye, irradiation time and number of piezoelectric were chosen as the input variables in this process. In addition, the efficiency of the dye's removal was considered as the response of the process. The variables were the most significant factors due to different processes of dye's removal in the literature. The factors were coded based on three levels as the low (-1), medium (0) and high (+1) with a central coefficient ($\alpha=2$). Range and coded levels are reported in Table 1. Thirty experimental runs were randomly selected as the design of experiments according to the CCD approach.

4.1.2. Quadratic regression model and analysis of variance (ANOVA)

The RSM suggested a quadratic model due to the lowest error in predicting the experimental data than other models (linear, cubic, power, log and etc.). An exact model can be effective in decreasing the number of experiments, subsequently the cost and time parameters. Therefore it is essential to develop a good model for estimating the results. Finally, a quadratic regression equation was introduced as the best model in terms of coded factors as follows:

$$R = +47.89 + 7.27A + 0.8615B - 3.78C + 0.6895D - 0.7468AC + 0.9517AD + 0.9307CD + 8.32A^2 - 1.79B^2 - 4.25C^2 - 2.33D^2 \quad (2)$$

Table 1. The coded levels of the variables and the experiments based on the CCD method.

Variables	Factor code	Levels				
		-2	-1	0	+1	+2
pH	A	1.5	3	4.5	6	7.5
Irradiation time (min)	B	10	20	30	40	50
Initial concentration (mg/l)	C	5	10	15	20	25
Number of piezoelectric	D	1	2	3	4	5
Run	A	B	C	D	R%, exp	
1	0	-1	0	0	46	
2	2	2	1	-2	65	
3	2	-2	2	2	59	
4	1	-1	0	0	60	
5	0	-1	0	0	43	
6	1	0	-1	0	65	
7	0	0	0	0	51	
8	2	-2	-2	2	71	
9	-2	2	-2	-2	46	
10	0	0	0	-1	44	
11	-2	2	-2	2	33	
12	-1	0	0	0	47	
13	0	-1	1	0	37	
14	-2	-2	2	2	30	
15	2	-2	1	-2	62	
16	-2	-2	-2	2	29	
17	-2	2	2	-2	28	
18	2	2	-2	-2	73	
19	0	0	0	-1	44	
20	2	2	2	2	61	
21	-2	2	2	2	31	
22	-1	0	1	0	41	
23	1	0	0	-1	59	
24	0	0	1	0	41	
25	0	0	-1	0	49	
26	2	-2	-2	-2	68	
27	-2	-2	2	-2	26	
28	-2	-2	-2	-2	43	
29	0	0	-1	-1	45	
30	2	2	-2	2	78	

The model was modified by eliminating the non-significant variables in order to reach a brief model without excess calculations. The actual and predicted results are depicted in Figure 4. As shown in the Figure, it can be found that there is a superior agreement between the model and the experimental data.

The quadratic model not only clearly described the variables but indicated the interaction between the parameters. This model including; linear, interaction and second order variables which are significant in evaluating the effects on the dye's removal. For instance, Interactions between the variables investigate two variables in the process, simultaneously. The reported results in Table 2 determine the performance of the model through the statistical indicators. It is denoted that R^2 , adjusted R^2 and predicted R^2 are 0.99, 0.99 and 0.98, respectively. In other words, total variations could be explained by this model. Therefore, three important indicators confirmed accuracy and

generality of the model. In addition, the other indicators are in a proper condition. Furthermore, the quadratic model is a promising model in estimating the decolorization's efficiency from water and wastewater of the textile industry as a general model. Moreover, analysis of variance (ANOVA) was used to examine the predicted model. Linear, quadratic and interaction effects on the response were evaluated by the probability value (p-value). The variables with p-value less than 0.01 are highly significant, between 0.01 and 0.05, significant and higher than 0.05 are considered as non-significant effect in the statistical studies [42,43]. Table 3 reports that the model is significant for the efficiency of the dye's removal. In other words, the model is precise and reliable at 95% confidence level due to the data processing and rational variations regarding the variables which were used in this study. In addition, lack of fit index had non-significant degree (greater than 0.05). It verified the validity of the model. As tabulated in Table 3, the linear variables are in highly significant (A, B, C) and significant (D)

degrees for the R response. The ANOVA determined that the interaction's effects between the pH and the initial concentration of the dye (AC), the pH and number of piezoelectric (AD), also the initial concentration of the dye and number of piezoelectric (CD) have the highest significance among the other interactions. Moreover, the effects of the time-dependent interactions (AB, BC, BD) were negligible. The second-order variables of the pH (A^2) and the initial concentration of the dye (C^2) were observed as more important effects on the dye's removal than other second-order effects. It should be noted that the second-order variables of time (B^2) and number of piezoelectric (D^2) had importance's degree of significant and high significant, respectively. Therefore, to reduce the mathematical calculations, the effects of the time-dependent interactions can be removed from the model by accepting a low error (Eq. 2). Numerical optimization determined the efficiency of the dye's removal of 76.05% which had an error percent of 2.5 compared to the experimental value of 78%. The optimum response occurred at pH 7.5, irradiation time of 50 min, initial concentration of 5 mg/l and 5 transducers.

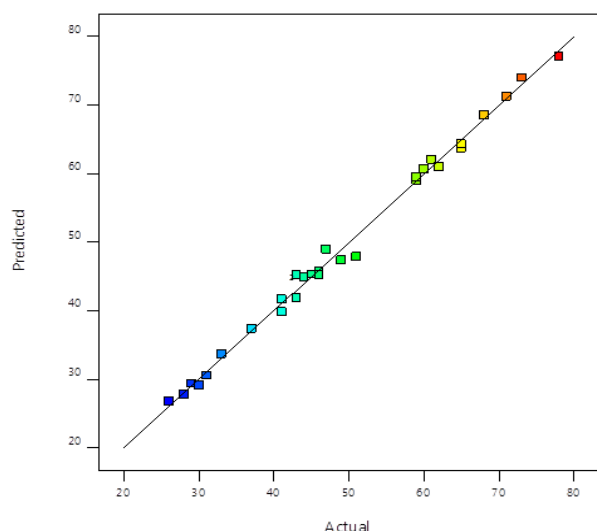


Fig. 4. Comparison between actual and predicted decolorization's efficiency.

Table 2. Statistical indicators of the developed model.

	R%
Standard deviation	1.54
R-Squared	0.99
Adj R-Squared	0.99
Pred R-Squared	0.98
Adeq Precision	46.23
Mean	49.17
C.V.% ¹	3.13

¹ Coefficient of Variation

4.1.3. The effects of the variables on the efficiency of the dye's removal

In this work, the operating parameters of the pH, irradiation time, initial concentration of the dye and number of transducer were investigated on removing the RR120 dye from aqueous solution at constant temperature of 25 °C. The pH is one of the important variables affecting on the processes of the dye's removal. Free radicals can show a better performance at specified range of the pH parameter. OH° attack on the dye's molecular at the cavity-water interface and bulk solution plays a vital role in decreasing the dye in the ultrasonic processes [45]. In this study, due to the poor performance of the process in the alkaline medium as well as the decrease in the number of tests, the acidic medium was selected. This is because the dye's molecules in the alkaline medium are ionized and tend to be hydrophilic in nature, subsequently are not separated from the solution [45]. Figure 5 shows the three dimensional response surface's plots. Each plot depicts the effect of two variables on the dye's removal at medium value of two other variables. In addition, increase the values are shown from blue to red.

Figure 5 (a, b) illustrates that increasing the pH to 4.5 has a negative effect and after this value an ascending trend occurs on the R response. It may be attributed to the performance of the ultrasonic waves in the specific frequency, power and the arrangement of the network in the production of the free radicals due to the related pH [46-48]. Enhancement of the time led to increase the R that is confirmed in Figure 5 (a). In fact, more time prepares an opportunity to contact between the ultrasonic waves and the RR120 dye' molecules [47,48]. In this work, maximum decolorization occurred within 50 min and was not shown any change after this time. Finally, the initial concentration of the dye had significant effect on the dye's removal. It can be found in Figure 5 (b) that the dye addition declined the decolorization's efficiency. In other words, more amount of the dye's molecular caused to increase the intermolecular forces of the solution at the constant frequency and power of the ultrasonic waves [48]. The positive effect of enhancing the piezoelectric is verified in Figure 5 (c). It was obviously observed that the ultrasonic waves in an appropriate phase and increasing waves acted as significant effects on the dye's removal. The reduction of the concentration through the ultrasonic waves can be discussed due to generate the ultrasonic's energy that may lead to decompose of the hydrocarbons' intermolecular bonds [37]. As demonstrated in Figure 5 (d, e, f), the interaction between the other parameters had same variations on the decolorization's efficiency of the RR120 dye based on the reasons mentioned above. Finally, The RSM confirmed the optimum conditions were attained at pH 7.5, time irradiation of 50 min, and initial concentration of 5 mg/l with 5 piezoelectrics.

Table 3. Analysis of variance and importance of variables in the quadratic regression model of the R.

Source	Sum of Squares	df ¹	Mean Square	F Value	p-value Prob > F	Degree of importance
Model	6118.55	14	437.04	184.05	< 0.0001	High significant
A-pH	2400.22	1	2400.22	1010.80	< 0.0001	High significant
B-Time	47.69	1	47.69	20.08	0.0004	High significant
C-Initial concentration	645.10	1	645.10	271.67	< 0.0001	High significant
D-Number of piezoelectric	20.08	1	20.08	8.46	0.0108	Significant
AB	2.61	1	2.61	1.10	0.3113	Non- significant
AC	90.62	1	90.62	38.16	< 0.0001	High significant
AD	156.29	1	156.29	65.82	< 0.0001	High significant
BC	7.36	1	7.36	3.10	0.0986	Non-significant
BD	0.1833	1	0.1833	0.0772	0.7849	Non-significant
CD	141.99	1	141.99	59.80	< 0.0001	High significant
A ²	318.89	1	318.89	134.29	< 0.0001	High significant
B ²	16.76	1	16.76	7.06	0.0179	Significant
C ²	128.88	1	128.88	54.27	< 0.0001	High significant
D ²	26.78	1	26.78	11.28	0.0043	High significant
Residual	35.62	15	2.37			
Lack of Fit	31.12	13	2.39	1.06	0.5843	Non- significant
Pure Error	4.50	2	2.25			
Cor Total	6154.17	29				

¹Degree of freedom

4.2. The ANN modeling and comparison with the RSM

As mentioned above, to more investigate of the RSM model, the ANN approach was applied. An exact estimation of the process' response is effective in reducing the time and cost parameters. The artificial intelligence can predict the complex processes at a high accuracy level. The Artificial neural networks (ANNs) as one of the subsets of the artificial intelligence used to model the decolorization's efficiency (R%). pH, irradiation time, initial concentration of the dye and number of piezoelectric were selected as the inputs of the network training. The R% was considered as the output of the process. The ranges of the data in the network training are according to Table 1. As discussed earlier, in the ANN, the number of inputs and outputs are chosen as the neurons of the input and output layers, respectively, while trial-and-error method determines the number of neurons in the hidden layer. Three important algorithms consist of Levenberg-Marquardt (LM), Bayesian-Regulation (BR) and Scaled Conjugate Gradient (SCG) was investigated to reach an optimum condition.

Figure 6 illustrates the optimum algorithm and the neurons of the hidden layer. As depicted in the figure, it can be found that the LM algorithm improves the network better than the BR and SCG algorithms. The LM algorithm by 4 neurons was selected in the optimization procedure due to the minimum

absolute average deviation (AAD) index. Although the BR by 5 neurons and the SCG by 8 neurons were also in an appropriate state, the response time and precision of the LM algorithm were superior in the network training. Finally the LM algorithm, the feed-forward back propagation type and optimum architecture (4-4-1) were obtained by the optimization of the network (Figure 7). Table 4 reports the training parameters of the network. The ANN makes the proper weights and biases and uses in an equation which is presented in Appendix A. The "tansig" and "purelin" were employed as transfer functions of the hidden and output layers, respectively.

Table 4. The ANN training parameters.

Parameters	Value
Network type	Feed-forward back propagation
Algorithm	Levenberg-Marquardt
Number of input nodes	4
Number of hidden neurons	4
Number of output nodes	1
Number of epochs	12
Validation checks	4
Mu	0.025

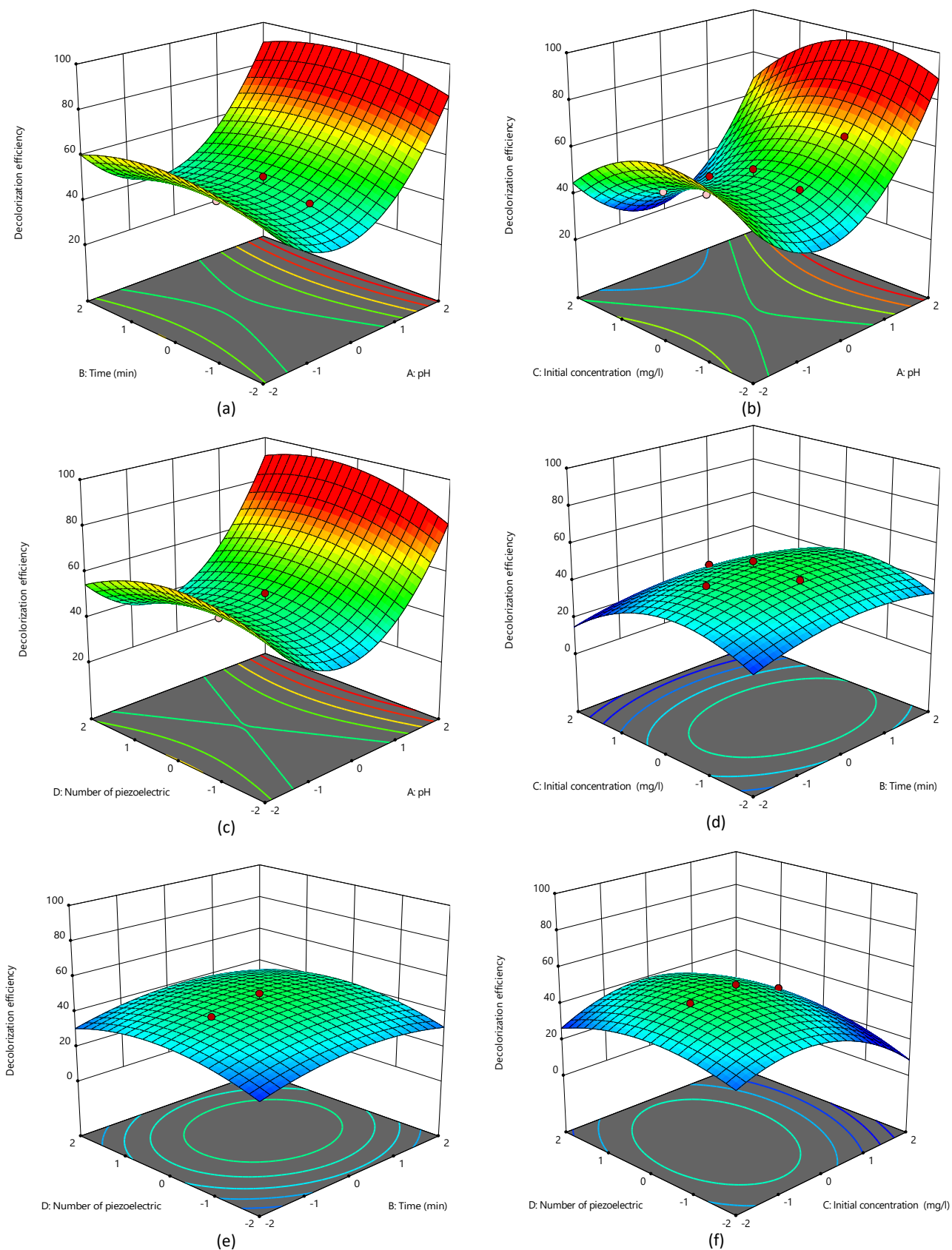


Fig. 5. The effects of variables on the R, a: pH and time, b: pH and initial concentration, c: pH and number of piezoelectric, d: time and initial concentration, e: time and number of piezoelectric, f: initial concentration and number of piezoelectric.

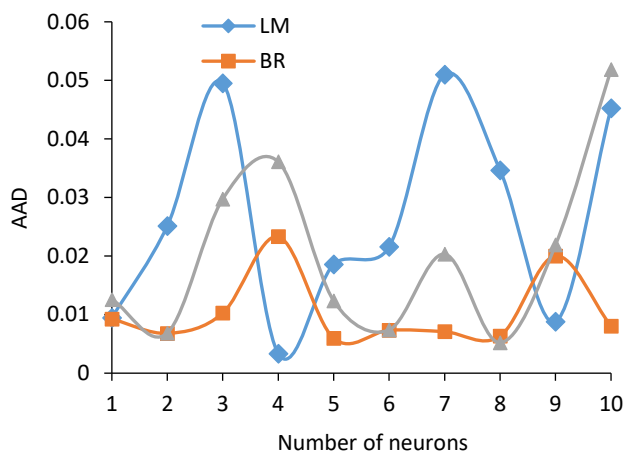


Fig. 6. Optimization of algorithms and neurons.

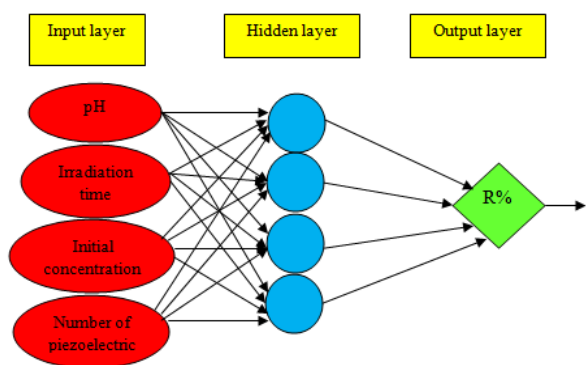


Fig. 7. Optimized ANN's architecture.

The results revealed that the R outputs were well predicted by the ANN model. Figure 8 shows the comparison between the ANN and RSM methods. It can be observed that the RSM predicts the R data better than the ANN. Moreover, as demonstrated in the figure, it can be mentioned that both the ANN and RSM have good agreement with the experimental data in forecasting the R output. Finally, the absolute average deviation (AAD), the average relative deviation (ARD) and total correlation coefficient (R^2) as performance's indicators numerically evaluated the accuracy of the RSM and ANN. Concerning to Table 5, the RSM has an exact performance with R^2 0.99, AAD 0.00 and ARD 0.01 in estimating the R. In summary, because of wide

applications and high confidence level of the ANN and RSM models, they can cover the mathematical models which need excess calculations with high errors. For instance, the ANN acts as a comprehensive information box so that the efficiency of the dye's removal is extracted by entering the input variables. In addition, both models can be used as general models in the textile industry.

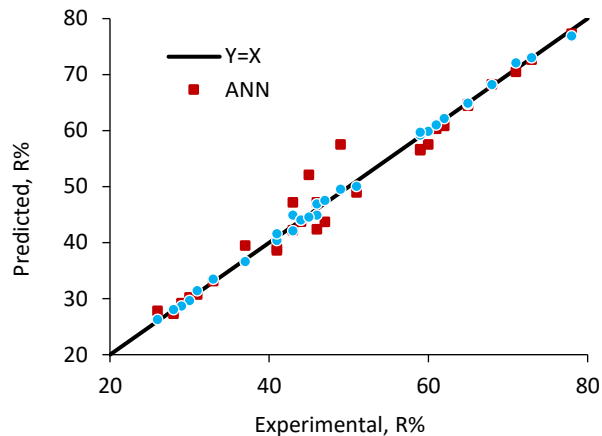


Fig. 8. The comparison between the developed approaches for R%.

Table 5. The performance of the ANN and RSM approaches.

Method	Performance indicators		
	AAD	ARD	R^2
RSM	0.00	0.01	0.99
ANN	0.00	0.04	0.97

4.3. The validation of the developed models

To validate the suggested models, ten additional experiments were carried out which had not been selected in the design of experiments. These experiments with their outputs are randomly reported in Table 6. Finally, the evaluation of the models was performed through the experiments. Table 7 reveals that ARD of 2.96 % and 5.22 % for the RSM and ANN, respectively, confirming a good prediction for the both models. It should be noted that the RSM developed the experimental data in a better accuracy. As mentioned earlier, it has been verified.

Table 6. Ten additional experiments to validate the developed models.

Number	pH	Irradiation time (min)	Initial concentration (mg/l)	Number of piezoelectric	R %
1	2	15	7	2	45
2	4	25	13	3	46
3	5	35	17	4	43
4	7	45	23	5	53
5	3.5	23	11	3	44
6	5.5	37	18	5	39
7	6.5	43	21	4	56
8	2.5	17	9	1	41
9	8	55	27	6	45
10	9	60	30	7	46

Table 7. The validation of the developed models.

Number	Experimental	The efficiency of the dye's removal (R)			
		Predicted(RSM)	Error (RSM)%	Predicted(ANN)	Error (ANN) %
1	45	46.93	-4.29	48.63	-8.07
2	46	44.47	3.33	45.55	0.98
3	43	44.29	-3	40.23	6.44
4	53	53.15	-0.28	55.15	-4.06
5	44	43.65	0.79	40.65	7.61
6	39	40.07	-5.45	41.47	-9.13
7	56	55.35	1.16	57.41	-2.52
8	41	39.17	4.46	40.89	0.27
9	45	48.42	-3.02	50.02	-6.43
10	46	49.03	3.86	47.56	6.75
ARD %			2.96	5.22	

5. Conclusions

The present work introduced a network of high frequency ultrasonic's transducers for removing the Reactive Red 120 dye from aqueous solution. The ultrasonic irradiation without additives played a significant role in cracking the hydrocarbon's bonds. The cavitation phenomenon and hydroxyl's radical attack were effective in decreasing the RR120 dye. The results showed that the ultrasonic decolorization's process had better performance in the acidic medium. In order to investigate the effects of the variables (pH, irradiation time, initial concentration of the dye and number of piezoelectric), the response surface methodology (RSM) was employed. Increasing the initial concentration had a negative effect on the R. Moreover, the piezoelectric addition aided to increase the dye's removal. The RSM not only developed an appropriate model but presented the analysis of variance (ANOVA) for the statistical investigation of the dye's removal. The performance's indices of the AAD, ARD and R² of 0.00, 0.01 and 0.99, respectively, verified a superior model in predicting the experimental data by the RSM. The maximum R% occurred at the removal's efficiency of 78% (pH 7.5, irradiation time of 50 min, initial concentration of 5 mg/l and number of transducer of 5) which was close to the model output (76.05%). The ANN developed another model to compare with the RSM. Performance's functions reported that the RSM was better than the ANN in predicting the R%. In this study, it is concluded that the network of the ultrasonic waves can be used as a safe, cost-effective, high quality and fast method in the dye's reduction of the wastewater in many industries.

Nomenclatures

ANN	Artificial neural network
AR	Analytical reagent
BBD	Box-Behnken design
CCD	Central composite design
C ₀	Initial concentration, mg/l
C	Final concentration, mg/l
Inc.	Incorporated
l	Liter
MHz	Mega Hertz
M _w	Molecular weight, g/mol
Purelin	Linear transfer function
R	The efficiency of the dye's removal
RR120	Reactive Red 120
RSM	Response surface methodology
Tansig	Tangent sigmoid transfer function
UV	Ultra violet
W	Watt

Appendix A

a) Quadratic model

$$Y = \alpha_0 + \sum_{i=1}^n \alpha_i X_i + \sum_{i=1}^n \alpha_{ii} X_i^2 + \sum_{i=1}^{n-1} \sum_{j=i+1}^n \alpha_{ij} X_i X_j + \varepsilon \quad (3)$$

b) ANN model

$$Y_j = f_t \left(\sum_{i=1}^n w_{ji} X_i + b_j \right) \quad (4)$$

c) Performance functions

$$AAD = \frac{1}{N} \sum_{i=1}^N \left(\frac{Y_{\text{exp},i} - Y_{\text{model},i}}{Y_{\text{exp},i}} \right)^2 \quad (5)$$

$$ARD = \frac{1}{N} \sum_{i=1}^N \left(\frac{|y_{exp,i} - y_{model,i}|}{y_{exp,i}} \right) \quad (6)$$

$$R^2 = \frac{\sum_{i=1}^N (y_{exp,i} - y_{model,mean})^2 - \sum_{i=1}^N (y_{exp,i} - y_{model,i})^2}{\sum_{i=1}^N (y_{model,mean} - y_{exp,i})^2} \quad (7)$$

References

- [1] schobanoglous, G., Burton, F., Stensel, H. D. (2003). Wastewater engineering: treatment and reuse. *Aufl. Boston: Hrsrg. Metcalf and Eddy Inc.???*
- [2] Singh, K. P., Gupta, S., Singh, A. K., Sinha, S. (2010). Experimental design and response surface modeling for optimization of Rhodamine B removal from water by magnetic nanocomposite. *Chemical engineering journal, 165*(1), 151-160.
- [3] Cheng, S., Zhang, L., Ma, A., Xia, H., Peng, J., Li, C., Shu, J. (2018). Comparison of activated carbon and iron/cerium modified activated carbon to remove methylene blue from wastewater. *Journal of environmental sciences, 65*, 92-102.
- [4] Merouani, S., Hamdaoui, O., Saoudi, F., Chiha, M., Pétrier, C. (2010). Influence of bicarbonate and carbonate ions on sonochemical degradation of Rhodamine B in aqueous phase. *Journal of hazardous materials, 175*(1-3), 593-599.
- [5] Galán, J., Rodríguez, A., Gómez, J. M., Allen, S. J., Walker, G. M. (2013). Reactive dye adsorption onto a novel mesoporous carbon. *Chemical engineering journal, 219*, 62-68.
- [6] Holkar, C. R., Jadhav, A. J., Pinjari, D. V., Mahamuni, N. M., Pandit, A. B. (2016). A critical review on textile wastewater treatments: possible approaches. *Journal of environmental management, 182*, 351-366.
- [7] Jain, R., Mathur, M., Sikarwar, S., Mittal, A. (2007). Removal of the hazardous dye rhodamine B through photocatalytic and adsorption treatments. *Journal of environmental management, 85*(4), 956-964.
- [8] Monash, P., Pugazhenth, G. (2009). Adsorption of crystal violet dye from aqueous solution using mesoporous materials synthesized at room temperature. *Adsorption, 15*(4), 390-405.
- [9] Moghaddam, S. S., Moghaddam, M. A., Arami, M. (2010). Coagulation/flocculation process for dye removal using sludge from water treatment plant: optimization through response surface methodology. *Journal of hazardous materials, 175*(1-3), 651-657.
- [10] Balla, W., Essadki, A. H., Gourich, B., Dassaa, A., Chenik, H., Azzi, M. (2010). Electrocoagulation/electroflotation of reactive, disperse and mixture dyes in an external-loop airlift reactor. *Journal of hazardous materials, 184*(1-3), 710-716.
- [11] Porter, J. J., Porter, R. S. (1995). Filtration studies of selected anionic dyes using asymmetric titanium dioxide membranes on porous stainless-steel tubes. *Journal of membrane science, 01*(1-2), 67-81.
- [12] Georgiou, D., Metallinou, C., Aivasidis, A., Voudrias, E., Gimouhopoulos, K. (2004). Decolorization of azo-reactive dyes and cotton-textile wastewater using anaerobic digestion and acetate-consuming bacteria. *Biochemical engineering journal, 19*(1), 75-79.
- [13] Ulson, S. M. D. A. G., Bonilla, K. A. S., de Souza, A. A. U. (2010). Removal of COD and color from hydrolyzed textile azo dye by combined ozonation and biological treatment. *Journal of hazardous materials, 179*(1-3), 35-42.
- [14] Yang, X., Wang, J., Zhao, X., Wang, Q., Xue, R. (2011). Increasing manganese peroxidase production and biodecolorization of triphenylmethane dyes by novel fungal consortium. *Bioresource technology, 102*(22), 10535-10541.
- [15] Carvalho, C., Fernandes, A., Lopes, A., Pinheiro, H., Gonçalves, I. (2007). Electrochemical degradation applied to the metabolites of Acid Orange 7 anaerobic biotreatment. *Chemosphere, 67*(7), 1316-1324.
- [16] Kansal, S. K., Singh, M., Sud, D. (2007). Studies on photodegradation of two commercial dyes in aqueous phase using different photocatalysts. *Journal of hazardous materials, 141*(3), 581-590.
- [17] Khataee, A. R., Safarpour, M., Zarei, M., Aber, S. (2012). Combined heterogeneous and homogeneous photodegradation of a dye using immobilized TiO₂ nanophotocatalyst and modified graphite electrode with carbon nanotubes. *Journal of molecular catalysis A: Chemical, 363*, 58-68.
- [18] Chakrabarti, S., Dutta, B. K. (2004). Photocatalytic degradation of model textile dyes in wastewater using ZnO as semiconductor catalyst. *Journal of hazardous materials, 112*(3), 269-278.
- [19] Khataee, A. R., Pons, M. N., Zahraa, O. (2009). Photocatalytic degradation of three azo dyes using immobilized TiO₂ nanoparticles on glass plates activated by UV light irradiation: Influence of dye molecular structure. *Journal of hazardous materials, 168*(1), 451-457.
- [20] Moon, B. H., Park, Y. B., Park, K. H. (2011). Fenton oxidation of Orange II by pre-reduction using nanoscale zero-valent iron. *Desalination, 268*(1-3), 249-252.
- [21] Karthikeyan, S., Titus, A., Gnanamani, A., Mandal, A. B., Sekaran, G. (2011). Treatment of textile wastewater by homogeneous and heterogeneous Fenton oxidation processes. *Desalination, 281*, 438-445.
- [22] Huang, Y. H., Huang, Y. F., Chang, P. S., Chen, C. Y. (2008). Comparative study of oxidation of dye-Reactive Black B by different advanced oxidation processes:

- Fenton, electro-Fenton and photo-Fenton. *Journal of hazardous materials*, 154(1-3), 655-662.
- [23] Papić, S., Vujević, D., Koprivanac, N., Šinko, D. (2009). Decolourization and mineralization of commercial reactive dyes by using homogeneous and heterogeneous Fenton and UV/Fenton processes. *Journal of hazardous materials*, 164(2-3), 1137-1145.
- [24] Aleksić, M., Kušić, H., Koprivanac, N., Leszczynska, D., Božić, A. L. (2010). Heterogeneous Fenton type processes for the degradation of organic dye pollutant in water the application of zeolite assisted AOPs. *Desalination*, 257(1-3), 22-29.
- [25] Sun, J. H., Sun, S. P., Wang, G. L., Qiao, L. P. (2007). Degradation of azo dye Amido black 10B in aqueous solution by Fenton oxidation process. *Dyes and pigments*, 74(3), 647-652.
- [26] Rosales, E., Pazos, M., Longo, M. A., Sanromán, M. A. (2009). Electro-Fenton decoloration of dyes in a continuous reactor: a promising technology in colored wastewater treatment. *Chemical engineering journal*, 155(1-2), 62-67.
- [27] Su, C. C., Pukdee-Asa, M., Ratanatamskul, C., Lu, M. C. (2011). Effect of operating parameters on the decolorization and oxidation of textile wastewater by the fluidized-bed Fenton process. *Separation and purification technology*, 83, 100-105.
- [28] Kansal, S. K., Singh, M., Sud, D. (2007). Studies on photodegradation of two commercial dyes in aqueous phase using different photocatalysts. *Journal of hazardous materials*, 141(3), 581-590.
- [29] Kasiri, M. B., Aleboyeh, H., Aleboyeh, A. (2008). Modeling and optimization of heterogeneous photo-fenton process with response surface methodology and artificial neural networks. *Environmental science and technology*, 42(21), 7970-7975.
- [30] Ahmed, S., Rasul, M. G., Martens, W. N., Brown, R., Hashib, M. A. (2011). Advances in heterogeneous photocatalytic degradation of phenols and dyes in wastewater: a review. *Water, air, and soil pollution*, 215(1), 3-29.
- [31] Chakrabarti, S., Dutta, B. K. (2004). Photocatalytic degradation of model textile dyes in wastewater using ZnO as semiconductor catalyst. *Journal of hazardous materials*, 112(3), 269-278.
- [32] Badr, Y., Abd El-Wahed, M. G., Mahmoud, M. A. (2008). Photocatalytic degradation of methyl red dye by silica nanoparticles. *Journal of hazardous materials*, 154(1-3), 245-253.
- [33] Ljubas, D., Smoljanić, G., Juretić, H. (2015). Degradation of Methyl Orange and Congo Red dyes by using TiO₂ nanoparticles activated by the solar and the solar-like radiation. *Journal of environmental management*, 161, 83-91.
- [34] Salari D, Niaeia A, Aberb S, Rasoulifard MH. (2009). The continuous photoreactor. *Journal of hazardous materials*, 166, 61-6.
- [35] lark, D., dos Reis Buzzo, A. J., Garcia, J. A. A., Côrrea, V. G., Helm, C. V., Corrêa, R. C. G., Peralta, R. M. (2019). Enzymatic degradation and detoxification of azo dye Congo red by a new laccase from *Oudemansiella canarii*. *Bioresource technology*, 289, 121655.
- [36] Kiayi, Z., Lotfabad, T. B., Heidarinassab, A., Shahcheraghi, F. (2019). Microbial degradation of azo dye carmoisine in aqueous medium using *Saccharomyces cerevisiae* ATCC 9763. *Journal of hazardous materials*, 373, 608-619.
- [37] Doust, A. M., Rahimi, M., Feyzi, M. (2015). Effects of solvent addition and ultrasound waves on viscosity reduction of residue fuel oil. *Chemical engineering and processing: Process intensification*, 95, 353-361.
- [38] Jaafarzadeh, N., Takdastan, A., Jorfi, S., Ghanbari, F., Ahmadi, M., Barzegar, G. (2018). The performance study on ultrasonic/Fe₃O₄/H₂O₂ for degradation of azo dye and real textile wastewater treatment. *Journal of molecular liquids*, 256, 462-470.
- [39] Shojaei, S., Nouri, A., Baharinikoo, L., Farahani, M. D., Shojaei, S. (2021). Removal of the hazardous dyes through adsorption over nanozeolite-X: Simultaneous model, design and analysis of experiments. *Polyhedron*, 196, 114995.
- [40] Shaikh, W. A., Islam, R. U., Chakraborty, S. (2021). Stable silver nanoparticle doped mesoporous biochar-based nanocomposite for efficient removal of toxic dyes. *Journal of environmental chemical engineering*, 9(1), 104982.
- [41] Swain, G., Singh, S., Sonwani, R. K., Singh, R. S., Jaiswal, R. P., Rai, B. N. (2021). Removal of Acid Orange 7 dye in a packed bed bioreactor: Process optimization using response surface methodology and kinetic study. *Bioresource technology reports*, 13, 100620.
- [42] Montgomery, D. C. (2017). *Design and analysis of experiments*. John Wiley and sons.
- [43] Myers RH, Montgomery DC. (2002) *Response surface methodology: Process and product optimization using designed experiments*. 2nd ed. USA: John Wiley and sons.
- [44] Demuth, H. B., Beale, M. H. (2000). *Neural network toolbox; for use with MATLAB; computation, visualization, programming; user's guide, version 4*. Math works.
- [45] Saharan, V. K., Badve, M. P., Pandit, A. B. (2011). Degradation of Reactive Red 120 dye using hydrodynamic cavitation. *Chemical engineering journal*, 178, 100-107.
- [46] Mahamuni, N. N., Adewuyi, Y. G. (2010). Advanced oxidation processes (AOPs) involving ultrasound for waste water treatment: a review with emphasis on

- cost estimation. *Ultrasonics sonochemistry*, 17(6), 990-1003.
- [47] Goel, M., Hongqiang, H., Mujumdar, A. S., Ray, M. B. (2004). Sonochemical decomposition of volatile and non-volatile organic compounds—a comparative study. *Water research*, 38(19), 4247-4261.
- [48] Ince, N. H., Tezcanli-Güyer, G. (2004). Impacts of pH and molecular structure on ultrasonic degradation of azo dyes. *Ultrasonics*, 42(1-9), 591-596.